Ab initio and density functional theory calculation of the structure and vibrational properties of n-vertex closo-carboranes, n=5, 6 and 7

ARTICLE *in* CHEMICAL PHYSICS · SEPTEMBER 2001

Impact Factor: 1.65 · DOI: 10.1016/S0301-0104(01)00420-7

3 AUTHORS, INCLUDING:

Michael S Deleuze
Hasselt University
132 PUBLICATIONS **2,673** CITATIONS

ELSEVIER

Chemical Physics 271 (2001) 17–30

Chemical Physics

www.elsevier.com/locate/chemphys

Ab initio and density functional theory calculation of the structure and vibrational properties of *n*-vertex *closo*-carboranes, $n = 5$, 6 and 7

A. Salam *, M.S. Deleuze, J.-P. François

Departement SBG and Institute for Materials Science (IMO), Limburgs Universitair Centrum, Universitaire Campus, B-3590 Diepenbeek, Belgium

Received 2 February 2001

Abstract

An extensive high-level computational study of various possible isomers of five, six and seven vertex *closo*-carboranes has been carried out using ab initio self-consistent field and density functional (DFT) theories. In total nine different cage structures have been investigated at the Hartree–Fock and B3LYP DFT levels in conjunction with the 6-31G** and 6-31++G** basis sets. Energies, optimized geometries, Mulliken charges, harmonic frequencies and electric dipole and quadrupole moments have been computed and compared with previous calculations and experimental data where applicable. The inclusion of diffuse functions in the basis set is shown not to significantly affect the results obtained for structural parameters and molecular properties. For a fixed cluster size, and for whichever model chemistry is chosen, the energetically most stable isomer is computed to be 1,5-$C_2B_3H_5$, 1,6-$C_2B_4H_6$ and 2,4-$C_2B_5H_7$. It is also found that irrespective of cluster vertex number, boron–hydrogen and carbon–hydrogen bond lengths remain relatively constant. The simulated vibrational spectra are analysed in detail and characteristic boron–hydrogen and carbon–hydrogen stretching frequencies and skeletal breathing modes are identified.

1. Introduction

Over the last 40 years in particular, boron and its chemistry [1–7] has attracted considerable interest from the chemical community and beyond. This has largely been due to boron's remarkable ability to compensate for its 'electron deficiency' by forming multicentre bonds in which three or more atoms are linked by a single electron pair. Interest has also been generated by the applications of boranes and carboranes, including their use in the treatment of specific forms of cancer in the boron neutron capture therapy (BNCT) of tumours [8], numerous industrial applications, and their widespread use in synthetic chemistry [6,9]. Another important recent application of borane and carborane cages, with varying degrees of success, has been as source compounds for the chemical vapour deposition of a variety of thin film materials [10] including variable band-gap boron carbide thin film semiconductors. For instance, boron carbide thin films with significantly increased resistivity have been successfully

* Corresponding author. Present address: Department of Chemistry and Biochemistry, Texas Tech University, P.O. Box 41061, Lubbock, TX 79409-1061, USA. Tel.: +1-806-742-3067; fax: +1-806-742-1289.

E-mail address: akbar@mailaps.org (A. Salam).

0301-0104/01/$ - see front matter
PII: S0301-0104(01)00420-7

fabricated from *nido*-pentaborane (B_5H_9) and methane using plasma-enhanced chemical vapour deposition [11–13], while the substituted carborane *nido*-2,3-diethyl-2,3-dicarbahexacarborane, $(C_2H_5)_2$-$C_2B_4H_6$, has been less successful as a source compound when undergoing synchrotron radiation induced deposition [14]. Angle-resolved photoemission measurements [15,16] have also been carried out on the second of these species and the results found to agree well with semiempirical modified neglect of diatomic overlap (MNDO) calculations. The electronic structure and spectroscopy of these compounds may be used to provide further information into the behaviour of the boron carbide family of semiconducting polytypes from which devices have been produced.

In this contribution, the structure and bonding of *n*-vertex *closo*-carboranes, $n = 5$, 6 and 7 will be investigated [17,18] using ab initio Hartree–Fock [19] and density functional theory (DFT) [20] calculations with a view to gaining further quantitative and chemical insight into the formation, relative stability, geometry and vibrational properties of these cluster compounds, which complement direct methods of structure elucidation such as X-ray and electron diffraction techniques and NMR spectroscopy. A similar study of 10 and 12 vertex *closo*-carboranes has also recently been performed [21]. Carboranes comprise a group of molecules, which from the perspective of multicentre bonding, are of considerable chemical interest. Even though many experimental and theoretical studies [4,5,17,22–36] of the bonding in heteroatom substituted boron clusters have been carried out, the complete structural data for clusters of even moderate size are still not available in the literature [17,18].

The structures of the first carboranes, 1,5-$C_2B_3H_5$, 1,2-$C_2B_4H_6$, 1,6-$C_2B_4H_6$ and 2,4-$C_2B_5H_7$ were deduced from ^{11}B NMR spectra, from which rules for carbon placement readily became apparent. Further experimental investigations performed on carboranes include inner-shell excitation spectroscopy [33,34], vibrational spectroscopy [37] in which the infrared (IR) and/or Raman spectra have been recorded and characterized, and photoelectron spectroscopy [25,28,29], which is one of the most powerful experimental techniques that has been applied to carboranes for the determination of electronic structure.

A large body of theoretical and computational work complements the various experimental studies of carboranes and include, inter alia, semiempirical (MNDO [15,16,23,24,29], Austin Model 1 (AM1) [27] and extended Hückel molecular orbital (EHMO) [26]), and ab initio [34,35] and DFT calculations [38] in which optimized geometrical structures, electronic properties and vibrational spectra have been computed. DFT, however, has not previously been used to investigate five, six and seven vertex *closo*-carboranes.

In this paper, results of calculations using ab initio HF and DFT on the various possible isomeric cage structures of $C_2B_3H_5$, $C_2B_4H_6$ and $C_2B_5H_7$ will be given with a view to providing qualitative and quantitative information on the structure and bonding in these electron deficient five, six and seven vertex species together with an analysis of their vibrational spectra. Following this introduction, a brief summary of the computational methods employed in this survey will be presented. In Section 3, results obtained for the energy, optimized bond lengths and molecular electric multipole moments as well as the Mulliken charges are given for all the compounds under investigation. An analysis of the computed vibrational spectra is carried out in Section 4 while the final section contains a brief summary of the results presented.

2. Computational methods

Before embarking on a comprehensive and systematic study of *n*-vertex *closo*-carborane cages, $n = 5$–7, a computational technique has to be chosen that is sufficiently accurate and yet at the same time not too demanding computationally. In addition, the preferred theoretical method should cope satisfactorily with the effects of electron correlation that are found to occur in the ground electronic state. Particularly favourable methods of calculation are the coupled-cluster ansatz including single and double excitations, with the contributions due to triple excitations estimated by perturbation theory, abbreviated as CCSD(T)

[39–41], which is used as a benchmark for most quantum chemical studies, or the complete active space with second-order perturbation theory (CASPT2) [42] method. For systems containing a large number of atoms however, both of these methods are untractable. In this regard, a method that is simultaneously accurate and affordable is DFT [20]. Recently [43,44], it has been demonstrated that DFT yields results that are similar in quality to those obtained using CCSD(T) for structural and electronic properties as well as for vibrational frequencies, for a wide range of chemical systems, if an appropriate functional and basis set is selected.

The calculations described in this study have been performed using the GAUSSIAN 98 [45] program running on a DEC 533 workstation and the GAUSSIAN 94 [46] package running on an IBM RS/6000 model 365 workstation at the Limburgs Universitair Centrum. Ab initio HF calculations were performed while the effects of electron correlation on the structure and vibrational spectrum were investigated by DFT calculations in conjunction with the B3LYP [47,48] exchange-correlation functional. The B3LYP functional consists of the Lee–Yang–Parr correlation functional [48], as well as the Vosko, Wilk, Nusair local correlation functional [49], in combination with a hybrid exchange functional first postulated by Becke [47]. The latter consists of a linear combination of the local density approximation, Becke's gradient correction [50], and the HF exchange energy based on Kohn–Sham orbitals [51]. Two standard basis sets [52] were used throughout, namely 6-31G** and 6-31++G**.

3. Results and discussion

3.1. Relative energy

Ab initio HF and DFT calculations were carried out on a total of nine isomers of five, six and seven apex *closo*-carborane cages comprising species 1,2-, 1,5- and 2,3-$C_2B_3H_5$, 1,2- and 1,6-$C_2B_4H_6$ and 1,2-, 1,7-, 2,3- and 2,4-$C_2B_5H_7$, and whose molecular structures are illustrated in Figs. 1–3, respectively. Results are given in Table 1 for the relative energy

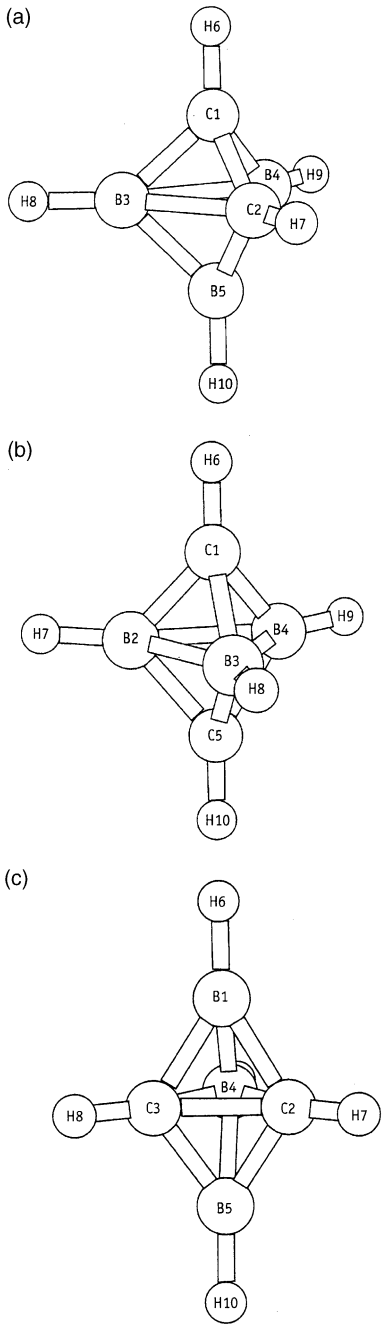

Fig. 1. The molecular structures of the three isomers of dicarba-*closo*-pentaborane: (a) 1,2-$C_2B_3H_5$, (b) 1,5-$C_2B_3H_5$ and (c) 2,3-$C_2B_3H_5$. Numerals indicate atomic centres.

of each isomer, for a fixed cluster size, calculated at the various levels of theory. Within a given level of

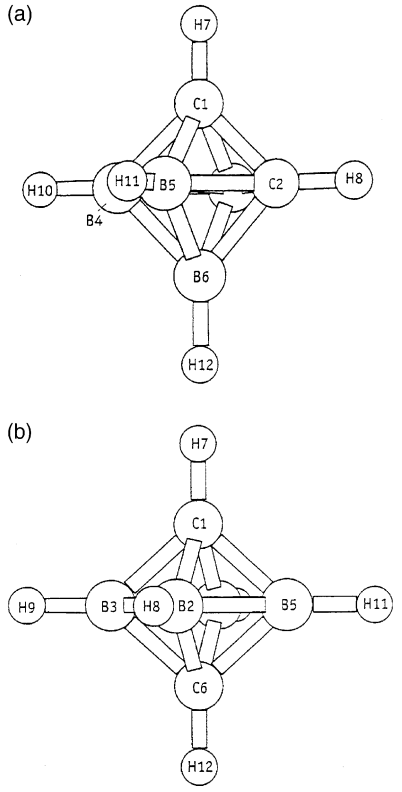

Fig. 2. The molecular structures of the two isomers of dicarba-*closo*-hexaborane: (a) 1,2-$C_2B_4H_6$ and (b) 1,6-$C_2B_4H_6$.

theory, the addition of diffuse functions to the 6-31G** basis set does not lead to any significant lowering in energy. Of the five and six vertex clusters studied, the most stable isomer is found to be 1,5-$C_2B_3H_5$ and 1,6-$C_2B_4H_6$ respectively; the former is 56.1 kcal mol^{-1} lower in energy than the 1,2-isomer, which in turn is 3.8 kcal mol^{-1} lower in energy than 2,3-$C_2B_3H_5$, while 1,6-$C_2B_4H_6$ is 13.8 kcal mol^{-1} lower in energy than its 1,2-analogue, at the B3LYP/6-31++G** model chemistry. The DFT calculated difference in energies between the two six vertex isomers is higher than the relative energy value obtained in a previous calculation [53] performed at the MP2/6-31G* level. The order of relative stabilities tends to support the conclusion that stability in these clusters is influenced largely by the relative positions assumed by the substituted carbon atoms. In the two lowest energy five and six vertex isomers, the carbon atoms adopt diametrically opposed positions in the cage structure, in what may be termed the 'para' form, in contrast to the other five and six vertex compounds. A similar structural trend was confirmed in a recent high-level quantum chemical study [21] of 10 and 12 vertex *closo*-carborane cages in which 1,10-$C_2B_8H_{10}$ and 1,12-$C_2B_{10}H_{12}$ were found to be the most stable clusters, respectively. On inspecting the results for the relative energies (at both the HF and B3LYP levels) of the seven vertex compounds, however, the property that the substituted carbon atoms be situated at opposite ends of the cage in the lowest energy structure, is not obeyed. Of the four seven vertex isomers considered, 2,4-$C_2B_5H_7$ is the most stable structure, while 1,7-$C_2B_5H_7$ is in fact the highest in energy. The predicted order of stabilities for *closo*-$C_2B_5H_7$ isomers is 2,4 > 1,2 $\sim$ 2,3 > 1,7 in slight disagreement with previous MP2/6-31G* calculations [53,54].

3.2. Optimized bond lengths

Presented in Table 2 are the bond lengths optimized at the highest theoretical level, namely B3LYP/6-31++G**, while Table 3 contains results for the total electric dipole moment, μ_{TOT}, and the components of the electric quadrupole moment, Q_{ij}, obtained at the same level of theory, for each isomer. Insignificant changes are found to occur in the optimized geometrical parameters and molecular properties when the basis set is improved by the inclusion of functions with diffuse character, as already noted when comparisons of energy were made. On examining the bond lengths in Table 2, it is found that for a fixed size cluster, the boron–carbon distance changes little, being approximately 1.56 Å for isomers with five vertices, $\sim$1.63 Å for isomers with six vertices and $\sim$1.5 and $\sim$1.8 Å for seven vertex species. A similar trend is observed for boron–boron bond distances in $n = 6$ and 7 apex cages, but which is in contrast to that found in the five vertex clusters, in which $r_{BB} = 1.64$ Å in the 1,2-isomer compared with 1.86 Å in the 1,5-species, and 1.66 Å in 2,3-$C_2B_3H_5$. Comparing boron–hydrogen and carbon–hydrogen bond lengths occurring in isomers of a particular cluster size, as well as between cages with differing number of vertices, r_{BH} and r_{CH} remain relatively constant, being approximately 1.18 and

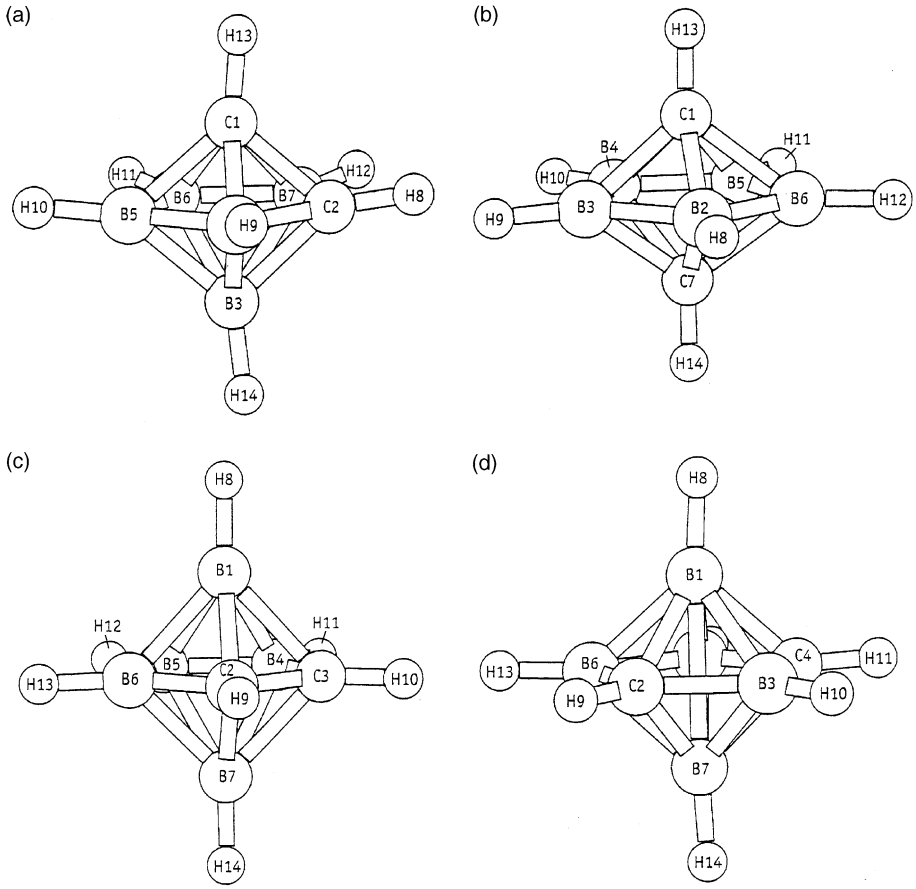

Fig. 3. The molecular structures of the four isomers of dicarba-*closo*-heptaborane: (a) 1,2-$C_2B_5H_7$, (b) 1,7-$C_2B_5H_7$, (c) 2,3-$C_2B_5H_7$ and (d) 2,4-$C_2B_5H_7$.

Table 1
Absolute energy (hartrees) and relative energies (kcal mol^{-1}) for *n*-vertex *closo*-carboranes, $n = 5$, 6 and 7, at different levels of theory (next to each species the symmetry of each isomer is given in parentheses)

Species	Theory			
	HF/6-31G**	HF/6-31++G**	B3LYP/6-31G**	B3LYP/6-31++G**
1,2-$C_2B_3H_5$ (C_s)	−152.5932	−152.5965	−153.6912	−153.6977
1,5-$C_2B_3H_5$ (D_{3h})	−63.3	−63.1	−56.2	−56.1
2,3-$C_2B_3H_5$ (C_{2v})	+12.0	+11.9	+3.7	+3.8
1,2-$C_2B_4H_6$ (C_{2v})	−177.9346	−177.9373	−179.2302	−179.2368
1,6-$C_2B_4H_6$ (D_{4h})	−12.9	−12.7	−14.2	−13.8
1,2-$C_2B_5H_7$ (C_s)	−203.1803	−203.1828	−204.6743	−204.6804
1,7-$C_2B_5H_7$ (D_{5h})	+33.9	+33.8	+25.1	+25.3
2,3-$C_2B_5H_7$ (C_{2v})	+0.8	+0.7	+1.8	+1.6
2,4-$C_2B_5H_7$ (C_{2v})	−46.7	−46.6	−41.4	−41.2

$\sim$1.08 Å respectively. Experimental bond lengths from X-ray diffraction measurements have been recorded for compounds 1,2- [55], 1,6-$C_2B_4H_6$ [56] and 2,4-$C_2B_5H_7$ [57]. For the first species,

Table 2
Bond lengths (Å) for five, six and seven vertex *closo*-carborane structures optimized at the B3LYP/6-31++G** theoretical level (see Figs. 1–3 for centre numbers)

1,2-$C_2B_3H_5$	C1–B3 = 1.558; C2–B3 = 1.906; B4–B5 = 1.636; B–H = 1.183; C–H = 1.085
1,5-$C_2B_3H_5$	C1–B3 = 1.555; B3–B4 = 1.858; B–H = 1.184; C–H = 1.078
2,3-$C_2B_3H_5$	B1–C2 = C3–B5 = 1.559; B1–H6 = B5–H10 = 1.177; B4–H9 = 1.179; B1–B4 = 1.658; C2–H7 = C3–H8 = 1.083
1,2-$C_2B_4H_6$	C1–B3 = C2–B3 = 1.631; B3–B4 = B3–B6 = 1.714; B–H = 1.180; C–H = 1.080
1,6-$C_2B_4H_6$	C1–B2 = B2–C6 = 1.625; B2–B3 = B3–B4 = 1.713; B–H = 1.178; C–H = 1.081
1,2-$C_2B_5H_7$	C1–C2 = 1.642; C2–B3 = 1.770; C1–B4 = C1–B7 = 1.759; C2–B4 = C2–B7 = 1.545; C1–B5 = C1–B6 = 1.717; B3–B4 = B3–B7 = 1.844; B3–B5 = B3–B6 = 1.790; B4–B5 = B6–B7 = 1.644; B5–B6 = 1.658; B4–H9 = B7–H12 = 1.183; B5–H10 = B6–H11 = B3–H14 = 1.182; C2–H8 = C1–H13 = 1.084
1,7-$C_2B_5H_7$	C–B(all equivalent) = 1.740; B–B(all equivalent) = 1.628; B–H(all equivalent) = 1.183; C–H(all equivalent) = 1.085
2,3-$C_2B_5H_7$	C2–C3 = 1.500; C3–B4 = 1.524; C2–B1 = 1.833; B4–B5 = B5–B6 = 1.548; B6–B7 = 1.862; B–H = 1.183; C3–H10 = C2–H11 = 1.083
2,4-$C_2B_5H_7$	C2–B1 = C2–B7 = C4–B1 = C4–B3 = 1.716; B1–B3 = B3–B7 = 1.841; B5–B6 = 1.651; C2–B3 = C4–B3 = 1.544; C4–B5 = C2–B6 = 1.566; B1–B5 = B5–B7 = B1–B6 = B6–B7 = 1.799; B3–H10 = B1–H8 = B7–H14 = 1.181; B5–H12 = B6–H13 = 1.182; C2–H9 = C4–H11 = 1.082

Table 3
Total dipole moment, μ_{TOT} (D) and principal axis components of the electric quadrupole moment matrix, Q_{ii} (DÅ) for five, six and seven vertex *closo*-carboranes calculated at the B3LYP/6-31++G** level of theory

Species	Property			
	μ_{TOT}	Q_{xx}	Q_{yy}	Q_{zz}
1,2-$C_2B_3H_5$	2.14	−29.6	−33.0	−32.0
1,5-$C_2B_3H_5$	0.0	−32.2	−32.2	−29.1
2,3-$C_2B_3H_5$	1.59	−28.1	−35.2	−31.0
1,2-$C_2B_4H_6$	2.25	−40.4	−36.3	−36.7
1,6-$C_2B_4H_6$	0.0	−40.1	−40.1	−32.8
1,2-$C_2B_5H_7$	2.43	−44.0	−41.9	−48.4
1,7-$C_2B_5H_7$	0.0	−48.1	−48.1	−37.8
2,3-$C_2B_5H_7$	3.46	−42.6	−47.2	−44.3
2,4-$C_2B_5H_7$	1.37	−45.6	−40.5	−47.2

Note: The only other non-vanishing components of the electric quadrupole tensor are $Q_{xy} = -2.7$ DÅ for 1,2-$C_2B_3H_5$, and $Q_{xy} = 0.6$ DÅ for 1,2-$C_2B_5H_7$.

$r_{C1B3} = 1.627$ Å, $r_{B3B6} = 1.721$ Å, compared with the theoretical values $r_{C1B3} = 1.631$ Å and $r_{B3B6} = 1.714$ Å. For the second compound, bond lengths of $r_{CB} = 1.633$ Å, $r_{BB} = 1.720$ Å have been measured, which compare extremely well with the B3LYP/6-31++G** values of $r_{CB} = 1.625$ Å and $r_{BB} = 1.713$ Å. For the 2,4-$C_2B_5H_7$ molecule the following bond lengths have been found on the experimental side: $r_{C2B3} = 1.546$, $r_{C2B6} = 1.563$ and $r_{C2B1} = 1.708$ Å and $r_{B5B6} = 1.651$, $r_{B1B3} = 1.818$ Å, compared to the theoretical values $r_{C2B3} = 1.544$, $r_{C2B6} = 1.566$, $r_{C2B1} = 1.716$ Å and $r_{B5B6} = 1.651$ and $r_{B1B3} = 1.841$ Å. Agreement between these data with computed equilibrium geometries is as good as can be expected, especially so for the seven vertex isomer.

3.3. Electric multipole moments and charge distribution

For those isomers whose dipole moment does not vanish due to symmetry, it is seen from Table 3 that as the number of vertices increases, the dipole moment of the 1,2-isomer increases steadily. Of the compounds with seven apexes, the 2,3-isomer has the largest polarity and 2,4-$C_2B_5H_7$ the smallest. The principal axis components of the electric quadrupole moment tensor of an isomer are seen to vary little for a fixed cluster size, but decrease as the size of the cage increases. The exceptions to the former trend are found in compounds with seven vertices; the *xx*-component of 1,7-$C_2B_5H_7$, the *yy*-components of 2,3- and 1,7- being noticeably lower than other values, while the *zz*-component is markedly higher in the 1,7-isomer when compared with other species in this family. One particularly interesting feature of the electric multipole moment data presented, is that for those species

whose dipole moment is zero, the *xx*- and *yy*-components of the electric quadrupole moment of a specific isomer are equal and considerably more negative than the corresponding *zz*-component. This occurs in 1,5-$C_2B_3H_5$ in which $Q_{xx} = Q_{yy} = -32.2$ DÅ, $Q_{zz} = -29.1$ DÅ; in 1,6-$C_2B_4H_6$ where $Q_{xx} = Q_{yy} = -40.1$ DÅ, $Q_{zz} = -32.8$ DÅ, and in 1,7-$C_2B_5H_7$ where it is seen that $Q_{xx} = Q_{yy} = -48.1$ DÅ, $Q_{zz} = -37.8$ DÅ, where the values reported have been calculated at the B3LYP/6-31++G** theoretical level. In these compounds the relative magnitudes of the principal axis components of the electric quadrupole moment matrix indicate elongation of spherical symmetry along the *x*- and *y*-directions and a compensatory shortening along the *z*-axis, the two carbon atoms being located on this third axis in each of these cases. This provides additional support for the conclusions obtained earlier regarding the importance of the relative positions of substituted carbon atoms on relative cluster stability through the degree of distortion of polyhedral symmetry. Further evidence is provided by the Mulliken atomic charges for each isomer calculated at the B3LYP/6-31++G** theoretical level and tabulated in Table 4. The symmetric distribution of charge in 1,5-$C_2B_3H_5$, 1,6-$C_2B_4H_6$ and 1,7-$C_2B_5H_7$, the 'para' forms, is clear: equal large negative charge is associated with the two carbon atoms (decreasing with increasing cage size) with equal small positive charge being attached to bonding hydrogens, while positive charge is evenly distributed amongst the boron

Table 4
B3LYP/6-31++G** evaluated Mulliken charges for five, six and seven vertex *closo*-carborane cluster species

1,2-$C_2B_3H_5$		1,5-$C_2B_3H_5$		2,3-$C_2B_3H_5$	
Centre	Charge	Centre	Charge	Centre	Charge
C1	−0.129	C1,C5	−0.297	B1,B5	0.159
C2	−0.326	B2–B4	0.191	C2,C3	−0.303
B3,B5	0.132	H6,H10	0.103	B4	0.189
B4	0.170	H7–H9	−0.061	H6,H10	−0.099
H6,H9	−0.061			H7,H8	0.180
H7	0.124			H9	−0.064
H8	0.135				
H10	−0.115				
1,2-$C_2B_4H_6$		1,6-$C_2B_4H_6$		1,2-$C_2B_5H_7$	
C1,C2	−0.301	C1,C6	−0.324	C1	−0.430
B3,B5	0.116	B2–B5	0.167	C2	−0.194
B4,B6	0.152	H8–H11	−0.064	B3	0.015
H7,H8	0.143	H7,H12	0.118	B4,B7	0.141
H9,H11	−0.063			B5,B6	0.143
H10,H12	−0.047			H8	0.176
				H9,H12	−0.072
				H10,H11	−0.064
				H13	0.163
				H14	−0.028
1,7-$C_2B_5H_7$		2,3-$C_2B_5H_7$		2,4-$C_2B_5H_7$	
C1,C7	−0.452	B1,B7	0.065	B1,B7	0.239
B2–B6	0.212	C2,C3	−0.295	C2,C4	−0.316
H8–H12	−0.080	B4,B6	0.139	B3	0.043
H13,H14	0.124	B5	0.177	B5,B6	0.013
		H9,H10	0.143	H9,H11	0.148
		H11,H13	−0.082	H10	−0.039
		H12	−0.092	H12,H13	−0.050
		H8,H14	−0.013	H8,H14	−0.036

atoms with small negative charge evenly shared amongst the hydrogens bonded to them. It should also be noted that equal negative charge is distributed on the two carbon atoms in 2,3-$C_2B_3H_5$, 1,2-$C_2B_4H_6$, and 2,3-$C_2B_5H_7$ and 2,4-$C_2B_5H_7$, in marked contrast to 1,2-$C_2B_3H_5$ and 1,2-$C_2B_5H_7$. This may be rationalized by consideration of the coordination numbers of the various carbon centres in the contrasting species. In 2,3-$C_2B_3H_5$, 1,2-$C_2B_4H_6$, 2,3- and 2,4-$C_2B_5H_7$, each carbon atom is pentacoordinate, having three boron and one carbon atom as nearest neighbours in the first two compounds, three boron and one carbon, and four boron atoms as next nearest neighbours in the last two molecules, respectively. In 1,2-$C_2B_3H_5$ however, carbon 1 is tetracoordinated and carbon at centre 2 is five coordinate, while in 1,2-$C_2B_5H_7$ carbon 1 has a coordination number of 6 and the other carbon is pentacoordinate, being immediately surrounded by four and three boron atoms, respectively.

4. Vibrational spectra

To further aid the analysis and understanding of the structure of five, six and seven vertex *closo*-carboranes, the vibrational spectra of these species were simulated by calculating vibrational frequencies and IR intensities. Displayed in Figs. 4–6 are the vibrational spectra computed at the B3LYP/6-31++G** theoretical level for the five, six and seven vertex species considered in this study, while Tables 5–7 contain corresponding values of the harmonic frequency, symmetry assignment, IR intensity, and zero-point vibrational energy. The calculated vibrational frequencies and zero-point energies have been scaled by a factor of 0.96, the recommended value for frequencies computed using DFT in which the B3LYP functional is used [58]. Whichever theoretical method was chosen, HF or DFT, changing basis sets by including functions of a diffuse nature made no significant difference to the calculated value of the vibrational frequency; in the majority of cases identical frequencies resulted, or differed, by at most, a few wave numbers. This again confirms the previously noted observation that addition of diffuse functions to a basis set produces insignificant changes in the structural and molecular properties

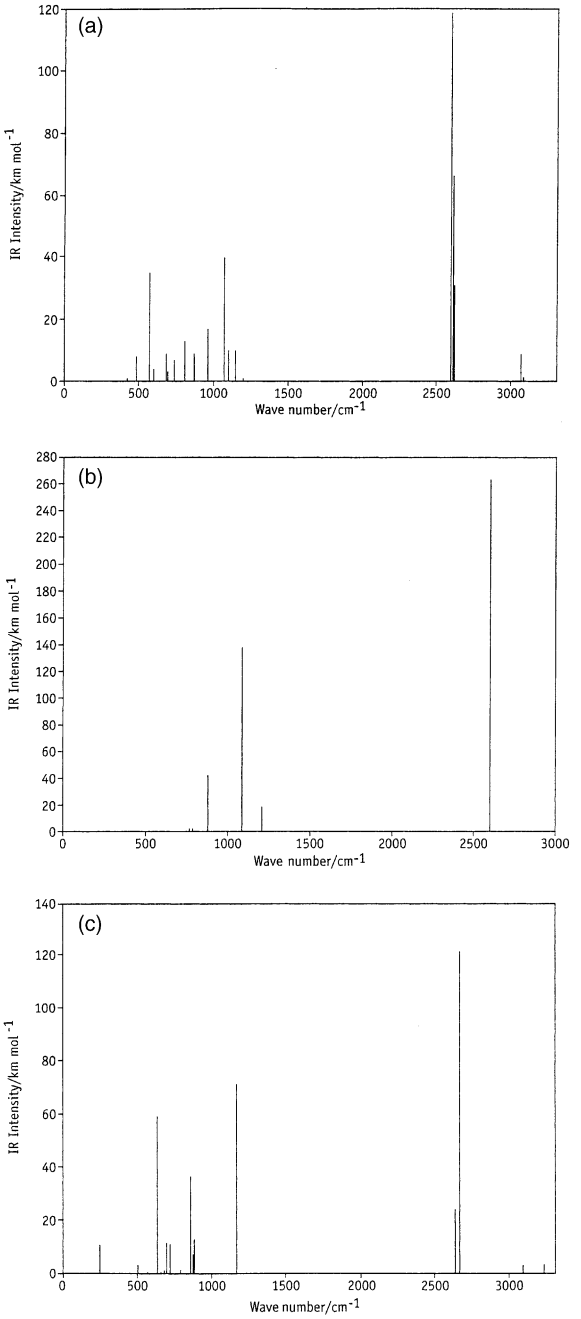

Fig. 4. B3LYP/6-31++G** calculated vibrational spectra (IR intensity (km mol^{-1}) versus wave number (cm^{-1})), for (a) 1,2-$C_2B_3H_5$, (b) 1,5-$C_2B_3H_5$ and (c) 2,3-$C_2B_3H_5$.

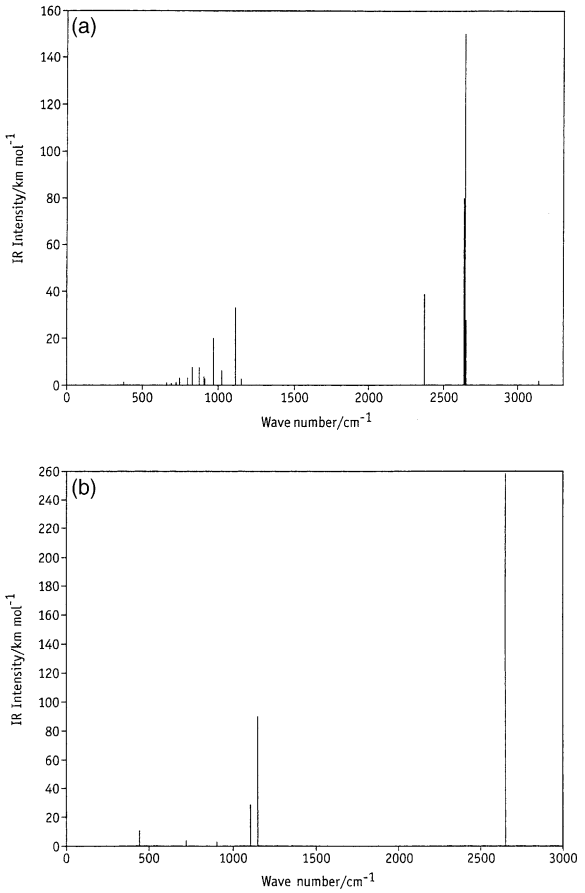

Fig. 5. B3LYP/6-31++G** calculated vibrational spectra (IR intensity (km mol^{-1}) versus wave number (cm^{-1})) for (a) 1,2-$C_2B_4H_6$ and (b) 1,6-$C_2B_4H_6$.

under investigation in small *closo*-carborane species.

The calculated vibrational spectra for the three *closo*-carborane isomers with five vertices are shown in Fig. 4, and are seen to have remarkable similarities and differences. The spectrum of 1,5-dicarba-*closo*-pentaborane is the simplest of the three, since this molecule has the higher symmetry, D_{3h} as opposed to the 1,2-isomer which belongs to the C_s point group and 2,3-$C_2B_3H_5$, which has C_{2v} symmetry. The C–H stretching frequency occurs at a wave number of 3096 cm^{-1} in the 1,2-isomer, at 3163 cm^{-1} (but with near zero IR intensity) for the 1,5-species, and at 3093 and 3105 cm^{-1} for the 2,3-species. The experimentally determined [59] C–H stretching frequency of the 1,5-compound is located at 3158 cm^{-1}. Of all the *closo*-carborane clusters, ranging from small to large cages, it is only in 1,5-$C_2B_3H_5$ that both the carbon atoms are in sites with a coordination number of 4, resulting in the highest C–H stretching frequency of any carborane. The electron withdrawing power of the whole carborane framework is reduced in 1,5-$C_2B_3H_5$ relative to the other species. All the peaks associated with C–H vibrations, however, are of very low intensity. Around 2600 cm^{-1} are seen the very intense lines arising from B–H stretching modes, occurring at 2601 cm^{-1} (intensity = 119 km mol^{-1}), 2618 cm^{-1} (67 km mol^{-1}) for the 1,2-species, and at 2609 cm^{-1} (264 km mol^{-1}) for the 1,5-isomer, and at 2673 cm^{-1} for the 2,3-compound; the corresponding experimentally [60] measured value for the 1,5-molecule being 2590 cm^{-1}. Bands appearing near 1200 cm^{-1} (1204 cm^{-1} for 1,2-$C_2B_3H_5$, 1208 cm^{-1} for the 1,5-isomer, and at 1170 cm^{-1} for 2,3-$C_2B_3H_5$) with low intensity are due to C–H deformation modes. The intense lines found at 880 cm^{-1} (intensity 42 km mol^{-1}) and 1091 cm^{-1} (138 km mol^{-1}) in the 1,5-$C_2B_3H_5$ spectrum are due to cage stretches and are located at 890 and 1119 cm^{-1} respectively in the recorded spectrum [59,61]. The analogous skeletal breathing modes in the 1,2-spectrum are located at 867 and 1070 cm^{-1}, although due to the lower symmetry of this molecule, many more lines appear in this spectral profile, not all of which may be assigned unambiguously.

Of the small *closo*-carborane species, extensive spectral investigations [61,62] have been carried out on the octahedral entity 1,6-dicarba-*closo*-hexaborane (D_{4h} symmetry), whose simulated spectra are illustrated in Fig. 5 (see also Table 6), along with that of the 1,2-isomer (C_{2v} point group). The two spectra are again remarkably similar to each other and to the vibrational spectra calculated for the five vertex clusters. Especially simple is the spectrum of the 1,6-compound. Located at 2657 cm^{-1} is the high-intensity (258 km mol^{-1}) peak due to B–H stretching, and which occurs at 2664 cm^{-1} in the measured spectrum. Not shown is the very weak C–H stretching mode found at 3130 cm^{-1}, which compares with an experimentally determined value of 3107 cm^{-1}. Lines measured [62] at

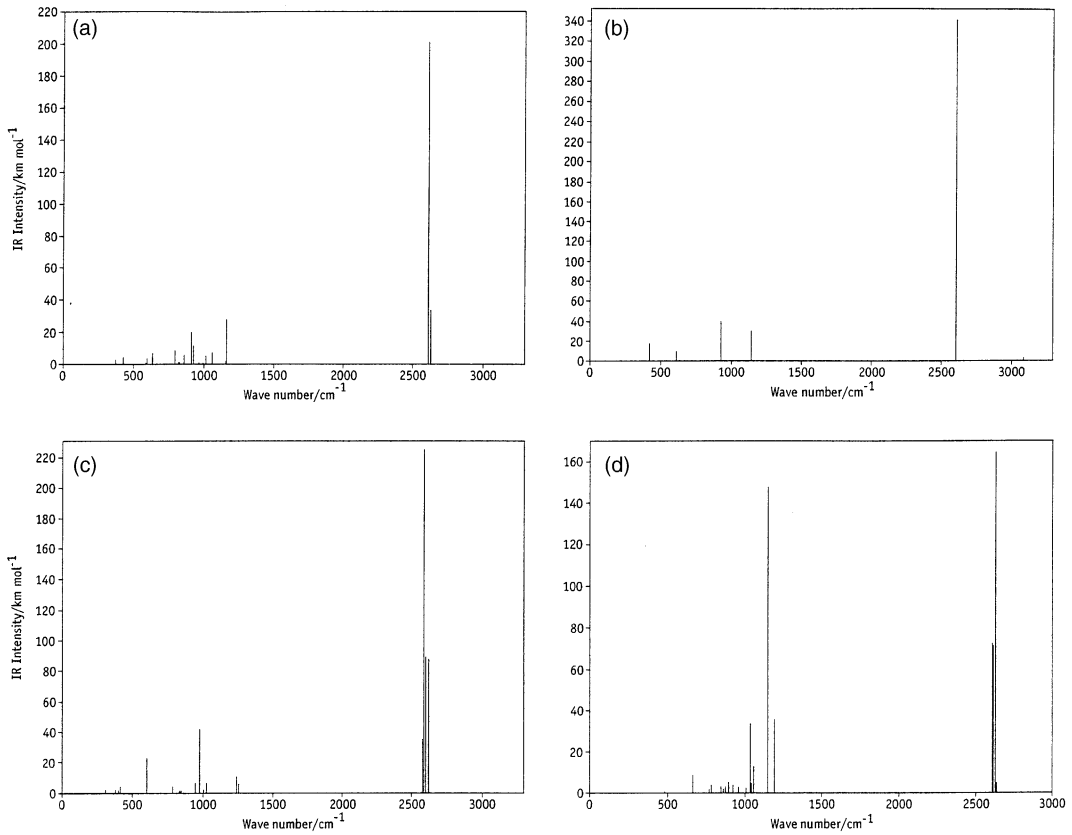

Fig. 6. B3LYP/6-31++G** calculated vibrational spectra (IR intensity (km mol^{-1}) versus wave number (cm^{-1})) for (a) 1,2-$C_2B_5H_7$, (b) 1,7-$C_2B_5H_7$, (c) 2,3-$C_2B_5H_7$ and (d) 2,4-$C_2B_5H_7$.

Table 5
Harmonic frequencies (cm^{-1}) and zero-point energy (kcal mol^{-1}) scaled by a factor of 0.96, and IR intensities (km mol^{-1}) for 1,2-$C_2B_3H_5$, 1,5-$C_2B_3H_5$ and 2,3-$C_2B_3H_5$ evaluated at the B3LYP/6-31++G** level of theory

Harmonic frequencies (cm^{-1})	Zero-point energy (kcal mol^{-1})
1,2-$C_2B_3H_5$ (C_s) 424(a″,1), 426(a′,0.6), 484(a″,8), 567(a′,35), 600(a′,4), 687(a″,9), 699(a′,3), 704(a″,0.3), 740(a′,7), 777(a″,0.2), 806(a′,13), 867(a′,9), 870(a″,7), 942(a″,0.6), 961(a′,17), 1070(a″,40), 1099(a′,10), 1146(a′,10), 1204(a′,1.2), 2601(a′,119), 2618(a″,67), 2627(a′,31), 3077(a′,9), 3096(a′,1.4)	41.59
1,5-$C_2B_3H_5$ (D_{3h}) 520(e′,0), 520(e′,0), 613(e″,0), 613(e″,0), 748(a_2',0), 756(e″,0), 756(e″,0), 764(a_2'',2), 790(e′,1), 790(e′,1), 814(a_1',0), 880(e′,21), 880(e′,21), 957(e″,0), 957(e″,0), 1091(e′,69), 1091(e′,69), 1122(a_1',0), 1208(a_2'',19), 2609(e′,132), 2609(e′,132), 2624(a_1',0), 3161(a_1',0), 3163(a_2'',0.15)	42.94
2,3-$C_2B_3H_5$ (C_{2v}) 225(b_2,0.2), 256(a_2,10.5), 510(b_1,3.2), 579(a_1,0.7), 638(b_2,59), 661(b_1,0.4), 687(a_1,1.1), 700(b_2,11.5), 727(b_1,11), 732(a_2,0), 795(a_1,1.4), 860(b_2,36.5), 880(a_1,7.3), 888(b_1,12.7), 892(a_2,0), 1170(b_2,71.7), 2641(a_1,24.2), 2673(b_2,121.5), 2675(a_1,0.1), 3093(b_1,3.2), 3105(a_1,4)	40.43

Table 6
Harmonic frequencies (cm^{-1}) and zero-point energy (kcal mol^{-1}) scaled by a factor of 0.96, and IR intensities (km mol^{-1}) for 1,2-$C_2B_4H_6$ and 1,6-$C_2B_4H_6$ evaluated at the B3LYP/6-31++G** level of theory

Harmonic frequencies (cm^{-1})	Zero-point energy (kcal mol^{-1})
1,2-$C_2B_4H_6$ (C_{2v})	
380(b_2,1), 413(a_2,0), 438(a_1,0.2), 664(b_1,1), 685(a_2,0), 694(a_1,0.6), 725(b_2,1), 750(b_1,3.2), 757(a_2,0), 778(a_1,0.2), 802(b_1,3), 828(a_1,9.5), 829(a_2,0), 838(b_2,0.2), 855(a_1,0.4), 879(b_1,8.7), 906(b_2,5), 910(a_1,3.4), 934(a_2,0), 973(b_2,20), 1028(a_1,6), 1118(b_1,45), 1147(a_1,0.2), 1154(b_2,2.4), 2374(a_1,39), 2634(b_2,90), 2642(b_1,150), 2652(a_1,28), 3134(b_2,2), 3143(a_1,0.1)	51.94
1,6-$C_2B_4H_6$ (D_{4h})	
371(b_{2u},0), 440(e_u,5.2), 440(e_u,5.2), 585(b_{2g},0), 709(e_u,0.1), 709(e_u,0.1), 725(a_{2u},3.2), 757(e_g,0), 757(e_g,0), 774(b_{2g},0), 811(a_{2g},0), 819(e_g,0), 819(e_g,0), 827(b_{1g},0), 855(b_{2u},0.4), 907(e_u,1.3), 907(e_u,1.3), 950(a_{1g},0), 983(e_g,0), 983(e_g,0), 1069(a_{1g},0), 1110(a_{2u},28), 1153(e_u,45), 1153(e_u,45), 2649(b_{1g},0), 2657(e_u,129), 2657(e_u,129), 2666(a_{1g},0), 3128(a_{1g},0), 3130(a_{2u},0.003)	52.18

Table 7
Harmonic frequencies (cm^{-1}) and zero-point energy (kcal mol^{-1}) scaled by a factor of 0.96, and IR intensities (km mol^{-1}) for 1,2-$C_2B_5H_7$, 1,7-$C_2B_5H_7$, 2,3-$C_2B_5H_7$ and 2,4-$C_2B_5H_7$ evaluated at the B3LYP/6-31++G** level of theory

Harmonic frequencies (cm^{-1})	Zero-point energy (kcal mol^{-1})
1,2-$C_2B_5H_7$ (C_s)	
380(a′,3), 399(a″,0), 426(a′,0.6), 430(a″,4), 493(a′,0.3), 566(a″,0.2), 588(a″,0.9), 602(a′,4), 637(a′,7), 752(a″,0.2), 757(a′,0), 798(a″,9), 799(a′,7), 822(a′,1.4), 830(a″,1.2), 842(a″,0.5), 848(a′,0.2), 859(a″,0.4), 863(a′,5.5), 912(a′,19), 926(a″,0.7), 928(a′,11), 971(a′,0.6), 996(a″,0.9), 1016(a′,4.5), 1022(a″,0.7), 1059(a′,7), 1158(a′,2), 1164(a″,28), 2608(a″,0), 2611(a′,111), 2613(a′,69), 2615(a″,202), 2628(a′,33), 3075(a′,0.1), 3090(a′,0.3)	60.16
1,7-$C_2B_5H_7$ (D_{5h})	
369(e_2'',0), 369(e_2'',0), 373(e_2',0), 373(e_2',0), 424(e_1',8.6), 424(e_1',8.6), 589(e_1'',0), 589(e_1'',0), 617(a_2'',10), 736(e_2',0), 736(e_2',0), 744(e_1',0.1), 744(e_1',0.1), 812(e_2'',0), 812(e_2'',0), 812(e_1'',0), 812(e_1'',0), 875(a_2',0), 918(a_1',0), 926(a_2'',40), 982(a_1',0), 982(e_1',0.1), 982(e_1',0.1), 983(e_1'',0), 983(e_1'',0), 993(e_2',0), 993(e_2',0),1146(e_1',15), 1146(e_1',15), 2600(e_2',0), 2600(e_2',0), 2606(e_1',171), 2606(e_1',171), 2614(a_1',0), 3081(a_1',0), 3084(a_2'',3)	59.23
2,3-$C_2B_5H_7$ (C_{2v})	
309(a_1,2.7), 377(b_2,2.3), 399(a_2,0), 404(b_1,1.5), 414(b_1,5), 542(a_2,0), 601(b_1,23), 606(b_2,0), 627(a_1,0), 696(a_1,0), 722(a_2,0), 731(b_1,0.2), 783(a_1,4.5), 785(b_2,4.3), 833(b_2,2), 839(a_1,1.2), 845(b_1,0), 849(b_1,2), 852(a_2,0), 863(b_2,0.3), 952(a_1,6.7), 959(a_2,0), 980(b_1,42), 1005(a_1,2.6), 1026(b_2,6.7), 1071(a_1,0.6), 1213(a_1,0.2), 1244(b_2,11.2), 1258(b_2,6), 2587(a_1,35), 2598(b_2,225), 2606(a_1,88), 2634(b_1,87), 2636(a_1,1.8), 3093(b_2,0.01), 3101(a_1,0.7)	60.10
2,4-$C_2B_5H_7$ (C_{2v})	
424(b_2,0.2), 473(a_2,0), 481(a_1,1), 482(b_1,0.3), 604(b_1,0), 615(a_1,0), 625(a_2,0), 640(b_2,0.2), 662(b_1,9), 767(b_1,0), 771(a_1,2), 781(b_2,4), 807(a_2,0), 813(a_1,0.1), 839(b_1,0.2), 842(a_2,0), 844(a_1,2.7), 862(b_2,2), 877(b_1,3.2), 895(b_2,5), 921(a_1,4.2), 962(a_1,3.2), 1005(a_2,0), 1011(b_2,2.4), 1039(b_1,34), 1042(a_1,4.5), 1057(b_2,13.2), 1149(b_2,148), 1192(a_1,36), 2612(b_2,72), 2617(a_1,71), 2629(a_1,112), 2630(b_1,164), 2638(a_1,5), 3104(a_1,0.011), 3106(b_2,0.24)	61.21

1130 and 1159 cm^{-1} are attributed to skeletal breathing modes in this molecule and are located at 1110 and 1153 cm^{-1} respectively in the theoretically calculated spectrum. Many more lines appear in the spectrum for the 1,2-isomer, this being due to the lower symmetry compared with the 1,6-compound. Nevertheless, characteristic polyhedral breathing and C–H and B–H stretching modes are still clearly identifiable. The well characterized vibrational spectrum of the octahedral anionic *closo*-hexaborate $B_6H_6^{2-}$ has served as a useful aid in the interpretation of the spectra of six vertex *closo*-carboranes, the former being considered as a representative carborane parent compound. An

analogous process has been used [21] in a similar study of the vibrational spectra of large *closo*-carborane clusters, in which the fully characterized $B_{12}H_{12}^{2-}$ IR spectrum was used to further the understanding of vibrations taking place in 12 vertex *closo*-carborane molecules.

Computed vibrational spectra for the four seven vertex *closo*-carborane isomeric species are displayed in Fig. 6 (see also Table 7). Again the appearance of characteristic peaks due to cage vibrations, B–H and C–H stretches provide a clear fingerprint for this class of compounds. In the 2,4-isomer (C_{2v} symmetry), where comparison with experiment [61,63] is possible, the most intense line found in the simulated spectra associated with B–H stretching is at 2630 cm^{-1}, with C–H stretching at 3106 cm^{-1} (with near zero IR intensity) and for the skeletal breathing mode, at 895 cm^{-1}, all of which compare favourably with mean measured [37] values of 2633, 3096 and 889 cm^{-1} respectively. Several lines in fact occur in the interval 1000–800 cm^{-1} for the less symmetrical 2,4-isomer and may be attributed to cage stretches with higher frequencies more B–C in character while the lower are more B–B. 1,7-$C_2B_5H_7$ yields the least complicated spectral pattern, belonging to the highest molecular point group of the four isomers, D_{5h}, while the most number of lines appear in the spectrum of 1,2-$C_2B_5H_7$, it having the lowest symmetry, C_s. On comparing the vibrational spectrum of the 2,3-isomer with the 2,4-species, a very intense line at 1149 cm^{-1} due to deformation of the cage is visible in the spectrum of the latter compound and which is absent in the former spectrum, while no peaks are seen below 400 cm^{-1} in the 2,4-$C_2B_5H_7$ profile in contrast to that computed for the 2,3-compound, despite both molecules belonging to the same C_{2v} point group.

Cage rigidity manifests itself in the high frequencies of the cage deformation modes (1200–800 cm^{-1}) and the striking absence of frequencies lower than about 400 cm^{-1} (lower than 450 cm^{-1} in measured spectra) from the vibrational spectra of all the compounds studied (except for 2,3-$C_2B_3H_5$), irrespective of polyhedron size, reflecting the specific electronic structure of deltahedral *closo*-carborane clusters. On examining the B–H stretching frequencies of the most intense peaks in all of the carboranes investigated in the present work, and which lie at 2625 ± 30 cm^{-1}, no correlation with either cage size or boron coordination number is exhibited. This contrasts with the C–H stretching mode, whose frequency clearly depends on the coordination number of the carbon atoms. In 1,5-$C_2B_3H_5$ in which carbon is tetracoordinated, C–H stretching occurs at 3160 cm^{-1} as opposed to carborane species in which carbon has a coordination number of 5 and in which the C–H stretching frequency drops by about 50 wave numbers to around 3100 cm^{-1}, irrespective of cluster size. The C–H stretching frequency, although very weakly intense, is especially informative in the interpretation of carborane vibrational spectra, being extremely sensitive to all intramolecular effects. The low intensity of the peaks associated with C–H stretches indicate unusually high ionic character in these bonds, i.e. C^-–H^+, and reflect the strongly localized nature of the C–H vibrations. This leads to very minor alterations of the dipole moments in the case of the 'para' structures, namely those isomers in which the two carbon atoms are placed in directly opposite positions in the cage, since the antisymmetric stretches occur along the main symmetry axis. In the remaining clusters, the almost homopolar C–H bonds give rise to weakly intense bands. On the other hand, the large intensities seen for the B–H stretches are in line with the much more strongly delocalized nature of these vibrational modes.

5. Summary

Various possible isomeric forms of dicarba-*closo*-carborane cages $C_2B_{n-2}H_n$, $n = 5$–7 have been studied computationally. The chief theoretical methods employed have been DFT with the B3LYP functional and which have supplemented results obtained via ab initio HF calculations. Two standard basis sets, 6-31G** and 6-31++G**, have been used throughout. Energies, geometries, electric multipole moments, Mulliken charges and harmonic frequencies have been computed for nine different isomers at various theoretical levels and compared and contrasted with previous low-level

calculations, and where possible, with experimental data. The energetically most stable isomer for each sized cluster was found to be 1,5-$C_2B_3H_5$, 1,6-$C_2B_4H_6$ and 2,4-$C_2B_5H_7$, in agreement with earlier predictions of relative isomer stability. From the results of geometry optimizations over the series of molecules investigated, boron–hydrogen and carbon–hydrogen bond lengths were found to be very similar in magnitude, and on comparison with corresponding distances in large *closo*-carborane cages, 10 and 12 vertex species for instance [21], are seen to change little. The stretching frequencies associated with these bonds are clearly marked in the calculated vibrational spectra of these systems. Very low intensity bands assigned to C–H stretches are located near 3100 cm^{-1} while high-intensity lines due to B–H stretching modes occur at 2600 cm^{-1}. The particularly good agreement with measured spectra of these two characteristic features also holds with the identification of peaks at 700 cm^{-1} arising from polyhedral breathing modes.

This study complements recent computational work [21] on 10 and 12 vertex *closo*-carboranes.

Acknowledgements

AS acknowledges a postdoctoral grant from the "Bijzonder Onderzoeksfonds" (BOF) of the Limburgs Universitair Centrum (LUC). MSD is grateful to the FWO-Vlaanderen ("Fonds voor Wetenshappelijk Onderzoek van Vlaanderen") and to the BOF of the LUC.

References

[1] F.A. Cotton, G. Wilkinson, C.A. Murillo, M. Bochmann, Advanced Inorganic Chemistry, Wiley, New York, 1997 (Chapter 5).
[2] D.M.P. Mingos, D.J. Wales, Introduction to Cluster Chemistry, Prentice Hall, New Jersey, 1990.
[3] J.F. Liebman, A. Greenberg, R.E. Williams (Eds.), Advances in Boron and the Boranes, VCH, New York, 1988.
[4] G.A. Olah, K. Wade, R.E. Williams (Eds.), Electron Deficient Boron and Carbon Clusters, Wiley, New York, 1991.
[5] S. Hermanek (Ed.), Boron Chemistry (special issue), Chem. Rev. 92 (1992) 1.
[6] E. Abel, F.G.A. Stone, G. Wilkinson (Eds.), Comprehensive Organometallic Chemistry, Pergamon, Oxford, 1995.
[7] W. Siebert (Ed.), Advances in Boron Chemistry, Royal Society of Chemistry, Cambridge, 1997.
[8] J. Plesek, Chem. Rev. 92 (1992) 269.
[9] R.N. Grimes, Chem. Rev. 92 (1992) 251.
[10] F.C. Mattacotta, G. Ottaviani (Eds.), Science and Technology of Thin Films, World Scientific, Singapore, 1995.
[11] S. Lee, J. Mazurowski, G. Ramseyer, P.A. Dowben, J. Appl. Phys. 72 (1992) 4925.
[12] S. Lee, J. Mazurowski, W.L. O'Brien, Q.Y. Dong, J.J. Jia, T.A. Callcott, Y. Tan, K.E. Miyano, D.L. Ederer, D.R. Mueller, P.A. Dowben, J. Appl. Phys. 74 (1993) 6919.
[13] S. Lee, P.A. Dowben, Appl. Phys. A 58 (1994) 223.
[14] F.K. Perkins, M. Onellion, S. Lee, D. Li, J. Mazurowski, P.A. Dowben, Appl. Phys. A 54 (1992) 442.
[15] S. Lee, D. Li, P.A. Dowben, F.K. Perkins, M. Onellion, J.T. Spencer, J. Am. Chem. Soc. 113 (1991) 8444.
[16] S. Lee, P.A. Dowben, A.T. Wen, J. Vac. Sci. Technol. A 10 (1992) 881.
[17] P.v.R. Schleyer, K. Najafian, Inorg. Chem. 37 (1998) 3454.
[18] R.A. Beaudet, in: J.F. Liebman, A. Greenberg, R.E. Williams (Eds.), Advances in Boron and the Boranes, VCH, New York, 1988, p. 417.
[19] A. Szabo, N.S. Ostlund, Modern Quantum Chemistry, Dover, New York, 1996.
[20] R.G. Parr, W. Yang, Density Functional Theory of Atoms and Molecules, Oxford University Press, New York, 1989.
[21] A. Salam, M.S. Deleuze, J.-P. Francois, to be submitted.
[22] R.K. Bohn, M.D. Bohn, Inorg. Chem. 10 (1971) 350.
[23] M.J.S. Dewar, M.L. McKee, J. Am. Chem. Soc. 99 (1977) 5231.
[24] M.J.S. Dewar, M.L. McKee, Inorg. Chem. 19 (1980) 2662.
[25] T. Vondrak, Polyhedron 6 (1987) 1559.
[26] G.F. Mitchell, A.J. Welch, J. Chem. Soc. Dalton Trans. (1987) 1017.
[27] M.J.S. Dewar, C. Jie, E.G. Zoebisch, Organometallics 7 (1988) 513.
[28] T. Vondrak, J. Plesek, S. Hermanek, B. Stibr, Polyhedron 8 (1989) 805.
[29] P. Brint, B. Sangchakr, M. McGrath, T.R. Spalding, R.J. Suffolk, Inorg. Chem. 29 (1990) 47.
[30] R.E. Williams, Chem. Rev. 92 (1992) 177.
[31] V.I. Bregadze, Chem. Rev. 92 (1992) 209.
[32] B. Stibr, Chem. Rev. 92 (1992) 225.
[33] A.P. Hitchcock, A.T. Wen, S. Lee, J.A. Glass Jr., J.T. Spencer, P.A. Dowben, J. Phys. Chem. 97 (1993) 8171.
[34] A.P. Hitchcock, S.G. Urquhart, A. Wen, A.L.D. Kilcoyne, T. Tyliszczak, E. Rühl, N. Kosugi, J.D. Bozek, J.T. Spencer, D.N. McIlroy, P.A. Dowben, J. Phys. Chem. A 101 (1997) 3483.
[35] P.v.R. Schleyer, K. Najafian, Inorg. Chem. 37 (1998) 3454.
[36] T. Onak, J. Jaballas, M. Barfield, J. Am. Chem. Soc. 121 (1999) 2850.
[37] L.A. Leites, Chem. Rev. 92 (1992) 279.

[38] M.L. McKee, J. Am. Chem. Soc. 119 (1997) 4220.
[39] K. Raghavachari, G.W. Trucks, M. Head-Gordon, J.A. Pople, Chem. Phys. Lett. 157 (1989) 479.
[40] R.J. Bartlett, J. Phys. Chem. 93 (1989) 1697.
[41] T.J. Lee, E.G. Scuseria, in: S.R. Langhoff (Ed.), Quantum Mechanical Electronic Structure Calculations with Chemical Accuracy, Kluwer, Dordrecht, 1995.
[42] K. Andersson, P.Å. Malmqvist, B.O. Roos, A.J. Sadlej, K. Wolinski, J. Phys. Chem. 94 (1990) 5483.
[43] P.J. Stephens, F.J. Devlin, C.F. Chabalowski, M.J. Frisch, J. Phys. Chem. 98 (1994) 11623.
[44] J.M.L. Martin, J. El-Yazal, J.-P. François, Mol. Phys. 86 (1995) 1437.
[45] M.J. Frisch, G.W. Trucks, H.B. Schlegel, G.E. Scuseria, M.A. Robb, J.A. Cheeseman, V.G. Zakrzewski, J.A. Montgomery Jr., R.E. Stratmann, J.C. Burant, S. Dapprich, J.M. Millam, A.D. Daniels, K.N. Rudin, M.C. Strain, O. Farkas, J. Tomasi, M. Barone, M. Cossi, R. Cammi, B. Mennucci, C. Pomelli, C. Adamo, S. Clifford, J. Ochterski, G.A. Petersson, P.Y. Ayala, Q. Cui, K. Morokuma, D.K. Malick, A.D. Rabuck, K. Raghavachari, J.B. Foresman, J. Cioslowski, J.V. Ortiz, A.G. Baboul, B.B. Stefanov, G. Liu, A. Liashenko, P. Piskorz, I. Komarom, R. Gomperts, R.L. Martin, D.J. Fox, T. Keith, M.A. Al-Laham, C.Y. Peng, A. Nanayakkara, C. Gonzalez, M. Challacombe, P.M.W. Gill, B. Johnson, W. Chen, M.W. Wong, J.L. Andres, M. Head-Gordon, E.S. Replogle, J.A. Pople, GAUSSIAN 98, revision A.7, Gaussian, Pittsburgh, PA, 1998.
[46] M.J. Frisch, et al., GAUSSIAN 94, revision B.1, Gaussian, Pittsburgh, PA, 1995.
[47] A.D. Becke, J. Chem. Phys. 98 (1993) 5648.
[48] C. Lee, W. Yang, R.G. Parr, Phys. Rev. B 37 (1988) 785.
[49] S.J. Vosko, L. Wilk, M. Nusair, Can. J. Phys. 58 (1980) 1200.
[50] A.D. Becke, J. Chem. Phys. 88 (1988) 1053.
[51] W. Kohn, L.J. Sham, Phys. Rev. 140 (1965) 1133.
[52] M.J. Frisch, J.A. Pople, J.S. Binkley, J. Chem. Phys. 80 (1984) 3265.
[53] M.L. McKee, J. Am. Chem. Soc. 110 (1988) 5317.
[54] J.J. Ott, C.A. Brown, B.M. Gimarc, Inorg. Chem. 28 (1988) 4269.
[55] R.A. Beaudet, R.L. Poynter, J. Chem. Phys. 53 (1970) 1899.
[56] E.A. McNeill, K.L. Gallaher, F.R. Scholer, S.H. Bauer, Inorg. Chem. 12 (1973) 2108.
[57] R.A. Beaudet, R.L. Poynter, J. Chem. Phys. 43 (1965) 2166.
[58] M.W. Wong, Chem. Phys. Lett. 256 (1996) 391.
[59] I. Shapiro, C.D. Good, R.E. Williams, J. Am. Chem. Soc. 84 (1962) 3837.
[60] R.N. Grimes, J. Am. Chem. Soc. 88 (1966) 1895.
[61] R.W. Jotham, D.J. Reynolds, J. Chem. Soc. A (1971) 3181.
[62] J. Bragin, D.S. Urevig, M. Diem, J. Raman Spectrosc. 12 (1982) 86.
[63] T. Onak, G.B. Dunks, R.A. Beaudet, R.L. Poynter, J. Am. Chem. Soc. 88 (1966) 4622.